J Elast (2011) 105:253–269
DOI 10.1007/s10659-011-9302-0

Mindlin's Problem for a Halfspace Indented by a Flexible Plate

A.P.S. Selvadurai · N.A. Dumont

Received: 7 December 2010 / Published online: 2 February 2011

Abstract The paper deals with a contact problem for an isotropic elastic halfspace indented by a flexible circular plate and simultaneously subjected to a Mindlin-type axial force. The approach adopted is to solve the contact problem for the flexible circular plate and the elastic halfspace; this serves as the auxiliary solution to examine, via the Maxwell-Betti reciprocal theorem, the influence of the internal Mindlin force. The contact between the flexible plate and the elastic halfspace is solved using a variational approach. The net displacement of the flexible circular plate and the internal Mindlin force can be evaluated in analytical form. The result has applications to the in situ evaluation of the deformability characteristics of geologic media.

Keywords Contact mechanics · Anchor-flexible plate interaction · Mindlin force problem · Variational solution · Maxwell-Betti reciprocal theorem

Mathematics Subject Classification (2000) 45 · 74 · 65

1 Introduction

The determination of the deformability characteristics of geologic materials relies on two approaches: The first involves laboratory measurement of the parameters using samples recovered from a site and the second determines the parameters in situ. Laboratory testing methods use elemental tests that may not be representative of the bulk behaviour of the geologic material. In situ tests, on the other hand, are difficult to conduct and their interpretation

A.P.S. Selvadurai (✉)
Department of Civil Engineering and Applied Mechanics, McGill University, 817 Sherbrooke Street West, Montreal, QC, Canada H3A 2K6
e-mail: patrick.selvadurai@mcgill.ca

N.A. Dumont
Civil Engineering Department, Pontifical Catholic University of Rio de Janeiro, 22451-900 Rio de Janeiro, Brazil
e-mail: dumont@puc-rio.br

usually involves an inverse analysis of the field data. In field testing the deformability characteristics of intact rock masses are measured using plate load tests, which ensures that large volumes are tested to include fissures, micro-cracks and intrusions, all of which contribute to scale effects as compared to elemental testing carried out at a laboratory setting [4, 10]. As the sizes of the defects and inhomogeneities increase, the dimensions of the loading plate should also increase so that representative volume elements of the rock mass can be tested. With large plate loading tests, the forces necessary to induce measurable plate deflections are also large, making the procedure inconvenient. One method of providing the reactive force to the test plate involves the use of an anchorage-cable system: The Cable-Jacking Load Test is a procedure where a self-stressing system is used to perform the plate load test and was formally proposed by Zienkiewicz and Stagg [22]. The interpretation of the results of the cable-jacking load test to determine the elasticity parameters of the tested rock requires a theoretical relationship that links the applied load to the measured plate deflection. The solution customarily used is the classical result for the axisymmetric smooth indentation of an elastic halfspace by a rigid circular indenter with a flat base, given by Boussinesq [2] and re-examined by Harding and Sneddon [9] (see, e.g., [1]), who used integral transform techniques and the theory of dual integral equations to obtain the same result. Other exact and approximate results for the indentation of an isotropic elastic halfspace by test plates of various planforms indenting the halfspace in either smooth or frictionless contact are given by Galin [6], Uflyand [21], Selvadurai [14, 18] and Gladwell [7]. The classical solution for the indentation of the halfspace by a rigid indenter cannot be directly applied for the interpretation of the Cable-Jacking Load Test. First, the anchorage force causes an interaction with the surface indentation leading to a reduction in the test plate deflections that are dependent on the location of the anchorage force resultant. An analysis of the interaction between a rigid test plate and a concentrated internal anchor load was first given by Selvadurai [12]. The work was extended to include distributed anchor loads [13] and transverse isotropy of the geologic medium [16]. However, the idealization of the test plate as a rigid indentor is inappropriate in situations where the test plate can experience flexural deflections under the action of localized loading and with geomaterials that have high relative stiffness properties. Modelling the interaction between a flexible plate and an internally located anchor force is therefore a useful result for a more accurate examination of load test data. To develop such a result, it is necessary to solve the problem of the interaction between a flexible plate and an isotropic elastic halfspace. The complete analysis of this problem requires the solution of a set of integro-differential equations, which can only be achieved using computational techniques. In this paper we make use of a variational procedure for the solution of the contact problem for a flexible plate and an elastic halfspace developed by Selvadurai [15] that approximates the axisymmetric deflection of the plate by a kinematically admissible field. The variational solution to the interaction between the flexible plate and the elastic halfspace also serves as the auxiliary solution for the analysis of the interaction between the flexible plate and the internal anchor force through the application of the Maxwell-Betti reciprocal theorem. The paper presents the formal developments leading to the analysis of the interaction between the externally loaded flexible plate and an internal Mindlin force [11]. Results are shown for a rigid plate and compared with the ones given by a boundary element implementation. While the application illustrated in the paper is motivated by geomechanics, the work can be easily extended to the consideration of other contact problems involving indenters and nuclei of thermoelastic strain [3].

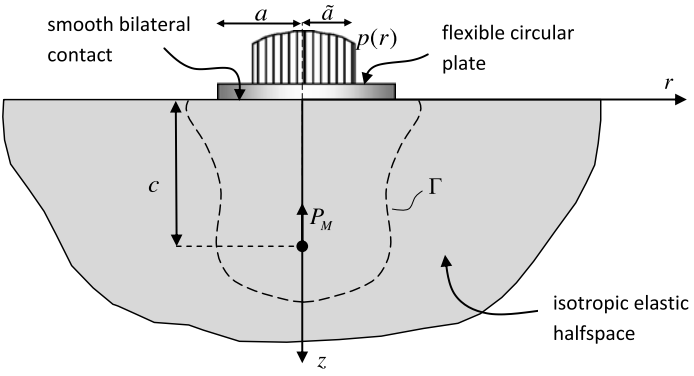

Fig. 1 The geometry of the interaction problem

2 The Interaction Problem

We consider the problem of the smooth contact between a flexible elastic plate and an isotropic elastic halfspace. The axisymmetric interaction between the plate and the halfspace is induced by external loads $p(r)$ applied to the flexible plate and an internal concentrated force P_M applied along the axis of symmetry (Fig. 1). In an actual test configuration, the external load $p(r)$ and the internal Mindlin force P_M form a self stressing loading system, which eliminates the need for an externally located reaction system. The flexural behaviour of the elastic plate is described by the Poisson-Kirchhoff-Germain thin plate theory and it is assumed that full contact is maintained over the contact region $0 \le r \le a$ during interaction. The boundary value problem that should be solved for the interaction between the plate and the elastic halfspace is given by Selvadurai [13, 17]:

$$D\nabla^2\nabla^2 w(r) + \frac{2G_S}{\pi(1-\nu_S)\,r}\frac{d}{dr}\int_0^r \frac{s}{\sqrt{s^2-r^2}}\left(\frac{d}{ds}\int_0^s \frac{r w(r)dr}{\sqrt{s^2-r^2}}\right)ds = p(r), \qquad (1)$$

where $D\,(= G_P h^3/6(1-\nu_P))$ is the flexural rigidity of the plate, G_i and ν_i are the constant shear modulus and Poisson's ratio of the elastic halfspace material $(i = S)$ and the plate material $(i = P)$ and ∇^2 is the radially symmetric form of Laplace's operator referred to the plane polar coordinate system. The Kirchhoff boundary conditions applicable to the plate are

$$M_{rr}(a) = -D\left(\frac{d^2w(r)}{dr^2} + \frac{\nu_P}{r}\frac{dw(r)}{dr}\right)_{r=a} = 0, \qquad Q_r(a) = -D\left(\frac{d}{dr}\nabla^2 w(r)\right)_{r=a} = 0, \qquad (2)$$

and the traction boundary conditions applicable to the surface of the halfspace are

$$\sigma_{zz}(r,0) = 0, \quad a < r < \infty; \qquad \sigma_{rz}(r,0) = 0, \quad 0 < r < \infty. \qquad (3)$$

In addition, the stress state in the halfspace should satisfy the global equilibrium condition

$$\oint\!\!\!\!\!\!\int_{\Gamma} \sigma_{ij} n_j \, d\Gamma + \left(2\pi\int_0^{\tilde{a}} p(r)\,dr - P_M\right)\delta_{i3} = 0, \qquad (4)$$

where Γ is a control surface that encompasses both the contacting plate and the internal Mindlin force and $\tilde{a}$ is the radius of the axisymmetric external load (Fig. 1). The result (4) is

used to determine the unknown maximum displacement of the indenting flexible plate. The complete solution of the mixed boundary value problem involving the integro-differential equation for $w(r)$ is particularly complicated because the equation cannot be integrated directly. Computational solutions to the stated mixed boundary value problem are certainly possible provided the range of results can cover the relative stiffness values of interest to practical application cases.

3 A Variational Approach

We consider the problem of the axisymmetric smooth indentation of the surface of the half-space by a plate of finite flexural rigidity. For the analysis of the problem we adopt the variational approach proposed by Selvadurai [15, 16] that makes use of the solution to the smooth indentation of the surface of a halfspace by an indentor of arbitrary axisymmetric profile, developed by Green [8] and Sneddon [20] (see also [7]). For the application of a variational approach, we assume that the deflected shape of the plate can be represented in the form of a power series in the radial coordinate, i.e.,

$$w(r) = a \sum_{n=0}^{m} C_n \left(\frac{r}{a}\right)^{2n}, \quad 0 \le r \le a, \tag{5}$$

with $m-1$ parameters C_n as the problem's unknowns, since two of them, say, C_{m-1} and C_m, must be chosen to satisfy *a priori* the Kirchhoff boundary conditions (2). The chosen form for the plate deflection gives continuous deflections, rotations and curvature in the plate region, which is necessary and sufficient for the application of the variational principle. The total potential energy functional of the plate-elastic halfspace region consists of the flexural energy of the plate, the elastic energy of the halfspace region and the potential energy of the applied loads. The flexural energy of the plate is given by

$$U_P = 2\pi D \int_0^a \left\{ [\nabla^2 w(r)]^2 - \frac{2(1-\nu_P)}{r} \frac{dw(r)}{dr} \frac{d^2 w(r)}{dr^2} \right\} r\, dr. \tag{6}$$

Since there is no loss of contact between the plate and the elastic halfspace, the contact is stationary and the strain energy of the halfspace region is consistent with the surface deflections defined by (5) and is given by

$$U_{HS} = \frac{2G_S}{(1-\nu_S)} \int_0^a w(r) \left\{ \frac{1}{r} \frac{d}{dr} \int_a^r \frac{s}{\sqrt{s^2 - r^2}} \left(\frac{d}{ds} \int_0^s \frac{r\, w(r)\, dr}{\sqrt{s^2 - r^2}} \right) ds \right\} r dr. \tag{7}$$

The total potential energy of the external loads is given by

$$U_L = -2\pi \int_0^{\tilde{a}} w(r) p(r) dr, \tag{8}$$

for the axisymmetric load $p(r)$ applied on a circle of radius $0 \le \tilde{a} \le a$. The total potential energy functional U for the plate-elastic medium system is given by

$$U = U_P + U_{HS} + U_L, \tag{9}$$

and for the total potential energy functional to satisfy the principle of stationary potential energy, we require $\delta U = 0$. Using the representation (5), the total potential energy functional for the plate-elastic medium system can be expressed in terms of $m-1$ independent

constants C_n $(n = 0, 1, \ldots, m-2)$. The principle of total potential energy requires that U be an extremum with respect to the kinematically admissible deformation field (5):

$$\frac{\partial U}{\partial C_n} = 0 \quad (n = 0, 1, \ldots, m-2). \tag{10}$$

This formally completes the analysis of the smooth axisymmetric interaction between the loaded flexible plate and the elastic halfspace and can be specialized to include a finite number of terms in the series (5). Once the displacements (5) are evaluated, the contact normal stress at the flexible plate-elastic halfspace interface can be obtained using the second term on the left hand side of (1):

$$\sigma_{zz}(r, 0) = \frac{2G_S}{\pi(1-\nu_S)r} \frac{d}{dr} \int_0^r \frac{s}{\sqrt{s^2 - r^2}} \left(\frac{d}{ds} \int_0^s \frac{r w(r) dr}{\sqrt{s^2 - r^2}} \right) ds. \tag{11}$$

Using the above expression for the contact stresses and Boussinesq's result for the loading of the surface of an elastic halfspace by a concentrated normal force [5], the displacement along the z-axis at a distance z can be evaluated as

$$u_z(0, z) = \frac{1}{2G_S} \int_0^a \frac{\sigma_{zz}(r, 0)}{\sqrt{r^2 + z^2}} \left(2(1-\nu_S) + \frac{z^2}{r^2 + z^2} \right) dr. \tag{12}$$

For $w(r)$ and $\sigma_{zz}(r, 0)$ given by (5) and (11), respectively, $\lim_{z \to 0} u_z(0, z) = w(0) = aC_0$.

4 Application of the Maxwell-Betti Reciprocal Theorem

The contact problem involving the flexible plate and the internal Mindlin force could also be formulated as one that also takes into consideration the energy of the internal Mindlin force. The approach adopted here is to solve the contact problem for the directly loaded flexible plate and the halfspace in the absence of the Mindlin force and then to use Maxwell-Betti reciprocal theorem to account for the additional changes to the plate deflections resulting from the internal Mindlin force. This avoids the tedious infinite domain integration of the stress field due to the Mindlin force. It is not possible to use the work of the Mindlin force at its point of application in computing the energy contribution since the axial displacement $u_z(0, z)$ is singular at the point of application of P_M.

We focus attention on the calculation of the displacement $w_r^{P_M}$ of the flexible plate at a radial distance r due to the application of the internal concentrated Mindlin force P_M located at a distance $z = c$ along the axis of symmetry. This can be approached as outlined in the previous Section but entails inordinately complicated manipulations involving the integrals occurring in the energy functional (9). Here we adopt a simpler procedure by applying the Maxwell-Betti reciprocal theorem. To apply the reciprocal theorem, we first develop, as an auxiliary solution, the result for the displacement at the point c of application of the Mindlin force due to a unit ring force,

$$P_r = \lim_{\Delta r \to 0} 2\pi \int_r^{r+\Delta r} p(\tilde{r}) \tilde{r} d\tilde{r} = 1, \tag{13}$$

applied at the distance r from the center of the flexible plate. Using the contact stresses $\sigma_{zz}^{P_r}$ given by (11) (which also accounts for the influence of plate flexibility on the contact

stresses) and Boussinesq's result (12), the corresponding axial displacement at a distance $z = c$ is

$$u_z^{P_r}(0,c) = w_c^{P_r} = \frac{1}{2G_S}\int_0^a \frac{\sigma_{zz}^{P_r}(r,0)}{\sqrt{r^2+c^2}}\left(2(1-\nu_S)+\frac{c^2}{r^2+c^2}\right)rdr. \tag{14}$$

For the application of the reciprocal theorem, and referring to Fig. 2, we assume that *complete bilateral* contact is maintained between the flexible elastic plate and the elastic halfspace, even though the contact is assumed to be *unbonded* and *frictionless*. The unknown displacement of the flexible plate at the distance r due to the internally applied Mindlin force is denoted by $w_r^{P_M}$. Since there are no frictional effects at the interface, the energy of the plate-elastic medium system is conservative. Also, since full bilateral contact is implicit in the formulation, the relationship between the loads and the corresponding displacements is linear. Therefore from the Maxwell-Betti reciprocal theorem, we have

$$P_r\, w_r^{P_M} = P_M\, w_c^{P_r}. \tag{15}$$

Taking into consideration the directions of the applied loads, the deflection of the flexible plate at a distance r during the combined application of the external concentrated load P_0 at

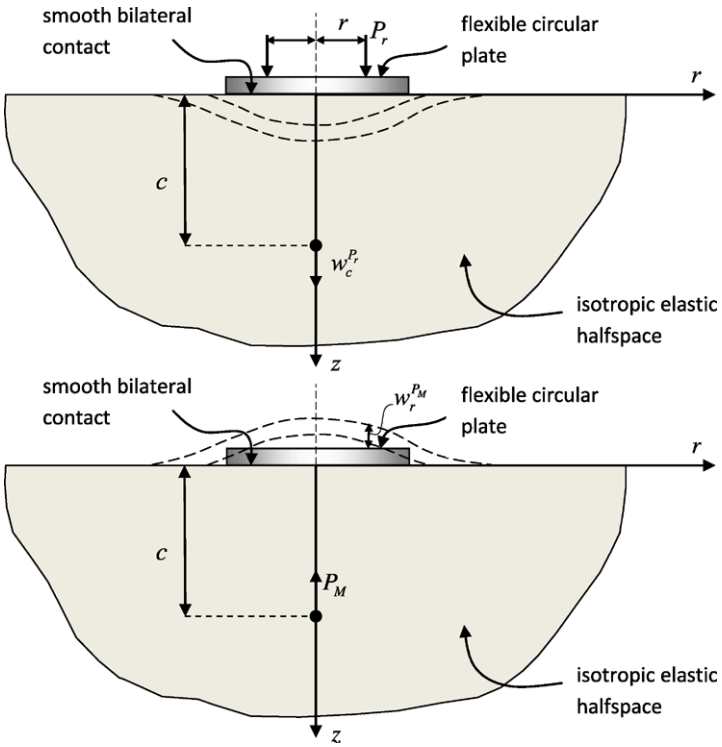

Fig. 2 The reciprocal states: (**a**) displacement $w_c^{P_r}$ at $(r = 0, z = c)$ due to a ring force P_r on the plate at $(r, z = 0)$; (**b**) displacement $w_r^{P_M}$ at $(r, z = 0)$ due to a point force P_M at $(r = 0, z = c)$

the center of the plate and the internal axial Mindlin force P_M is given by

$$w_r = w_r^{P_0} - \frac{P_M}{P_r} w_c^{P_r}, \tag{16}$$

where $w_r^{P_0}$ is given in (5) and $w_c^{P_r}$ is expressed in (14). The maximum deflection is given at $r = 0$. We can assess the consistency of assuming full contact between plate and soil by checking whether $\sigma_{zz}(r, 0) \leq 0$ for all $0 \leq r \leq a$ in (11) for $w(r) = w_r$ as obtained in (16). Such a consistency check can indeed be carried out; but due to the inordinate amount of algebraic manipulations involved, it is excluded from the presentation.

This formally completes the development of a variational approach for the analysis of the interaction between a flexible elastic plate and an isotropic elastic halfspace under the action of a Mindlin force. The accuracy of the approach depends on the number of terms in the series (5) used to represent the deflected shape of the plate. The ensuing section will investigate this aspect of the variational approach.

5 Matrix Implementation of the Proposed Variational Approach

Let $m - 1$ be the number of unknown parameters of the problem, obtained after introduction of the boundary conditions (2). Equation (1) is given in matrix format as

$$w(r) = \mathbf{wc} \equiv \mathbf{w}_0\mathbf{c}_0 + \mathbf{w}_1\mathbf{c}_1, \tag{17}$$

where $\mathbf{w}_0 = a[1, \xi^2, \xi^4, \ldots, \xi^{2m-2}]$ and $\mathbf{w}_1 = a[\xi^{2m}, \xi^{2m+2}]$, defined in terms of the natural coordinate $\xi = r/a$, are row vectors of dimension $m - 1$ and 2, respectively, and $\mathbf{c}_0$ and $\mathbf{c}_1$ are corresponding column vectors of parameters. Bold letters are used to characterize vectors (lower case) and matrices (capital case). The parameters $\mathbf{c}_1$ are evaluated in terms of $\mathbf{c}_0$ in such a way that the boundary conditions expressed by (2) are satisfied. For this purpose, (2) is written in matrix format as given in (A.1) of the Appendix, and $\mathbf{c}_1$ is evaluated as

$$\begin{Bmatrix} M_{rr}(a) \\ Q_r(a) \end{Bmatrix} = \mathbf{M}_0\mathbf{c}_0 + \mathbf{M}_1\mathbf{c}_1 = \mathbf{0} \quad \Rightarrow \quad \mathbf{c}_1 = -{\mathbf{M}_1}^{-1}\mathbf{M}_0\mathbf{c}_0 \equiv -\mathbf{T}\mathbf{c}_0, \tag{18}$$

with the introduction of the transformation matrix $\mathbf{T} = {\mathbf{M}_1}^{-1}\mathbf{M}_0$. Substituting for $\mathbf{c}_1$ back in (17), we obtain

$$w(r) = (\mathbf{w}_0 - \mathbf{w}_1\mathbf{T})\,\mathbf{c}_0, \tag{19}$$

where $\mathbf{c}_0$ are the $m - 1$ parameters to be evaluated.

However, it is more convenient to use in the subsequent developments the expression of $\mathbf{w}$ in (17) generated according to (5) and, just prior to applying the variational constraint indicated in (10), state that $\mathbf{c}$, according to (18), actually is

$$\mathbf{c} = \begin{bmatrix} \mathbf{I} \\ -\mathbf{T} \end{bmatrix} \mathbf{c}_0, \tag{20}$$

where $\mathbf{I}$ is the identity matrix of order $m - 1$. The energy expression (9), evaluated using all the $m + 1$ parameters $\mathbf{c}$, is given in matrix format as

$$U = \frac{1}{2}\mathbf{c}^{\mathrm{T}}\left[(\mathbf{K}_P + \mathbf{K}_{HS})\,\mathbf{c} - \mathbf{p}\right]. \tag{21}$$

Owing to the polynomial character of $w(r)$ in (5), a coefficient of the plate stiffness matrix obtained from (6),

$$\mathbf{K}_P = 2\pi D \int_0^a \left[\frac{\partial^2 \mathbf{w}^{\mathrm{T}}}{\partial r^2} \frac{\partial^2 \mathbf{w}}{\partial r^2} + \frac{1}{r^2} \frac{\partial \mathbf{w}^{\mathrm{T}}}{\partial r} \frac{\partial \mathbf{w}}{\partial r} + \frac{\nu_P}{r} \left(\frac{\partial \mathbf{w}^{\mathrm{T}}}{\partial r} \frac{\partial^2 \mathbf{w}}{\partial r^2} + \frac{\partial^2 \mathbf{w}^{\mathrm{T}}}{\partial r^2} \frac{\partial \mathbf{w}}{\partial r} \right) \right] r dr, \tag{22}$$

has the simple general expression (A.2).

The coefficients of the halfspace stiffness matrix $\mathbf{K}_{HS}$, introduced in (21) according to (7), cannot be generated by a simple algorithm, as above. However, formally, the matrix expression can be written as

$$\mathbf{K}_{HS} = \frac{4G_S}{(1-\nu_S)} \int_0^a \mathbf{w}^{\mathrm{T}} \left\{ \frac{1}{r} \frac{d}{dr} \int_a^r \frac{s}{\sqrt{s^2 - r^2}} \left(\frac{d}{ds} \int_0^s \frac{r\, \mathbf{w}\, dr}{\sqrt{s^2 - r^2}} \right) ds \right\} r dr. \tag{23}$$

In (A.3) we present results for $m = 7$, which is large enough for any practical numerical implementation.

The remaining term to be identified in (21) is the vector of equivalent forces $\mathbf{p}$ obtained from (8):

$$\mathbf{p} = 2\pi \int_0^{\tilde{a}} \mathbf{w}^{\mathrm{T}} p(r) dr. \tag{24}$$

Applying the boundary conditions according to (20) and (18), the energy expression (21) becomes

$$U = \frac{1}{2} \mathbf{c}_0^{\mathrm{T}} \left[\mathbf{I} - \mathbf{T}^{\mathrm{T}} \right] \left[(\mathbf{K}_P + \mathbf{K}_{HS}) \begin{bmatrix} \mathbf{I} \\ -\mathbf{T} \end{bmatrix} \mathbf{c}_0 - \mathbf{p} \right]. \tag{25}$$

Once $\mathbf{c}_0$ is solved from the system of equations

$$\left[\mathbf{I} - \mathbf{T}^{\mathrm{T}} \right] (\mathbf{K}_P + \mathbf{K}_{HS}) \begin{bmatrix} \mathbf{I} \\ -\mathbf{T} \end{bmatrix} \mathbf{c}_0 = \left[\mathbf{I} - \mathbf{T}^{\mathrm{T}} \right] \mathbf{p}, \tag{26}$$

the entire array of parameters $\mathbf{c}$ can be obtained from (20). We proceed to the evaluation of $w(r)$ in (17), with (11) and (14), and finally expressing w_r in (16), which gives the complete solution to the proposed problem. The contact stress $\sigma_{zz}(r, 0)$ in (11) is expressed in matrix format as

$$\sigma_{zz}(r, 0) = \frac{2G_S}{\pi (1 - \nu_S) \sqrt{1 - \xi^2}} \mathbf{s}\mathbf{c}, \tag{27}$$

where $\mathbf{s}$ is a row vector whose coefficients are polynomials in $\xi = r/a$. The matrix expression of $\mathbf{s}$ is given in (A.4) for $m = 7$ in (5).

The displacements (12) located at a point $(0, z)$ along the axis of symmetry may also be expressed in matrix format as

$$u_z(0, z) = \frac{z}{\pi} \left[2\mathbf{u}_1 + \frac{\mathbf{u}_2}{1 - \nu_S} \right] \mathbf{c}, \tag{28}$$

where $\mathbf{u}_1$ and $\mathbf{u}_2$ are transcendental functions of the natural variable $\epsilon = z/a$, as illustrated in (A.5) and (A.6) for the particular case of $m = 7$.

The net maximum deflection of the flexible plate during the combined application of the external concentrated load P_0 and the internal axial Mindlin force P_M is given in matrix

format, according to (16) and (28), by

$$w_0 = aC_0^{P_0} - \frac{P_M}{P_0}\frac{c}{\pi}\left[2\mathbf{u}_1 + \frac{\mathbf{u}_2}{1-\nu_S}\right]\mathbf{c}^{P_0}. \tag{29}$$

In this equation, $\mathbf{u}_1$ and $\mathbf{u}_2$ are evaluated for the particular case $z = c$ and $\mathbf{c}^{P_0}$ denotes the vector of constants $\mathbf{c}$ in (20) obtained after solution of $\mathbf{c}_0$ in (26) for the concentrated load P_0, such that

$$\left[\mathbf{I} - \mathbf{T}^{\mathrm{T}}\right]\mathbf{p} = P_0\begin{Bmatrix} a \\ \mathbf{0}\end{Bmatrix}. \tag{30}$$

In the above condensed vector of dimension $m-1$, only the first coefficient is non-zero. Observe that in (29) $C_0^{P_0}$ is the first parameter of (5), which corresponds to the first coefficient of the vector $\mathbf{c}^{P_0}$ solved in (26) for the load vector of (26) as in (30).

6 Specific Case of the Equations for $m = 3$

For purposes of illustration, specific results are presented in this section for $m = 3$ for the plate deflection defined by (5). The expression of $w(r)$ becomes

$$w(r) = a\left\{C_0 + C_2\left[\left(\frac{r}{a}\right)^2 + \lambda_1\left(\frac{r}{a}\right)^4 + \lambda_2\left(\frac{r}{a}\right)^6\right]\right\}, \quad [\lambda_1 : \lambda_2] = \frac{(1+\nu_P)}{2(2+\nu_P)}\left[-\frac{3}{2} : \frac{1}{3}\right]. \tag{31}$$

The expressions of the condensed stiffness matrices of (25) are

$$\mathbf{K}_P^c = \left[\mathbf{I} - \mathbf{T}^{\mathrm{T}}\right]\mathbf{K}_P\begin{bmatrix}\mathbf{I} \\ -\mathbf{T}\end{bmatrix} = \frac{8\pi D(7+9\nu_P+2\nu_P^2)}{(2+\nu_P)^2}\begin{bmatrix}0 & 0 \\ 0 & 1\end{bmatrix} \tag{32}$$

and

$$\mathbf{K}_{HS}^c = \left[\mathbf{I} - \mathbf{T}^{\mathrm{T}}\right]\mathbf{K}_{HS}\begin{bmatrix}\mathbf{I} \\ -\mathbf{T}\end{bmatrix} = \frac{4G_S a^3}{1-\nu_S}\begin{bmatrix}1 & \frac{106+36\nu_P}{105(2+\nu_S)} \\ \frac{106+36\nu_P}{105(2+\nu_S)} & \frac{1122124+694128\nu_P+112544\nu_P^2}{675675(2+\nu_S)^2}\end{bmatrix}. \tag{33}$$

Moreover, restricting attention to the case where the plate is subjected to a concentrated external load P_0, the vector of equivalent forces in (25) is given as in (30).

Then, the total potential energy functional for the loaded plate-elastic halfspace system can be evaluated in the form

$$U = \frac{2G_S a^3}{(1-\nu_S)}[C_0^2 + \chi_1 C_0 C_1 + \chi_2 C_1^2] + \pi\chi_3 D C_1^2 - P_0 a\, C_0, \tag{34}$$

where the expressions of χ_1, χ_2 and χ_3 are inferred from (32) and (33):

$$\left[\chi_1\ \chi_2\ \chi_3\right] = \left[\frac{(1-\nu_S)}{2G_S a^3}K_{HS_{12}}^c\ \ \frac{(1-\nu_S)}{4G_S a^3}K_{HS_{22}}^c\ \ \frac{1}{2\pi D}K_{P_{22}}^c\right]. \tag{35}$$

In (34), C_0 and C_1 are the coefficients of $\mathbf{c}_0$, which, evaluated from the condition that (25) is stationary, are expressed as

$$\mathbf{c}_0 = \frac{P_0 a}{K_{HS_{11}}^c(K_{P_{22}}^c + K_{HS_{22}}^c) - (K_{HS_{12}}^c)^2}\begin{Bmatrix}K_{P_{22}}^c + K_{HS_{22}}^c \\ -K_{HS_{12}}^c\end{Bmatrix}. \tag{36}$$

Finally, the expression for the deflection of the elastic plate can be written in the form

$$w(r) = \frac{P_0(1-\nu_S)}{2G_S a\,\Omega}\left(R\chi_3 + 2\chi_2 - \chi_1\left\{\frac{r^2}{a^2} + \lambda_1\frac{r^4}{a^4} + \lambda_2\frac{r^6}{a^6}\right\}\right), \tag{37}$$

where

$$\Omega = 2R\chi_3 + 4\chi_2 - \chi_1^2 \quad \text{and} \quad R = \frac{\pi\,(1-\nu_S)G_P}{6(1-\nu_P)G_S}\left(\frac{h}{a}\right)^3. \tag{38}$$

It may be noted that, as $R \to \infty$, the plate becomes rigid and (37) reduces to Boussinesq's classical result for the smooth indentation of an isotropic elastic halfspace by a rigid indentor with a flat base and a circular plan-form. The corresponding value of the indented displacement is

$$\lim_{D\to\infty} w(r) = \frac{P_0(1-\nu_S)}{4G_S a}. \tag{39}$$

The results for a plate with infinite stiffness are also obtained as a particular case of the implementation given in Sect. 4 if we use $m = 2$ in (5).

The contact normal stress at the flexible plate-elastic halfspace interface can be obtained using (37) and the second term on the left hand side of (1):

$$\sigma_{zz}(r,0) = \frac{P_0}{\pi\, a\,\Omega\sqrt{a^2-r^2}}\left(R\chi_3 + 2\chi_2 - \frac{\chi_1}{2}\sum_{i=0}^{3}\beta_i\left(\frac{r}{a}\right)^{2i}\right), \tag{40}$$

where

$$\beta_i = \left[-1 - \frac{4}{9}\lambda_1 - \frac{8}{25}\lambda_2,\, 2 - \frac{16}{9}\lambda_1 - \frac{16}{25}\lambda_2,\, \frac{32}{9}\lambda_1 - \frac{64}{25}\lambda_2,\, \frac{128}{25}\lambda_2\right]. \tag{41}$$

The total force on the indentor corresponds to P_0, irrespective of the flexibility of the plate. Again, as $R \to \infty$, (40) reduces to Boussinesq's result for the distribution of normal contact stresses at the base of a smooth rigid indentor.

For $m = 3$, the net maximum deflection of the flexible plate under the combined application of the external concentrated load P_0 and the internal axial Mindlin force P_0, according to (16), is

$$w_0 = w_0^{P_0} - \frac{P_M}{P_0}w_c^{P_0} = \frac{P_0(1-\nu_S)}{2G_s a\,\Omega}\left(R\chi_3 + 2\chi_2 - \frac{P_M}{\pi(1-\nu_S)P_0}\int_0^a \frac{r\,F(r)\,dr}{\sqrt{(a^2-r^2)(r^2+c^2)}}\right), \tag{42}$$

where

$$F(r) = \left(2(1-\nu_S) + \frac{c^2}{(r^2+c^2)}\right)\left(R\chi_3 + 2\chi_2 - \frac{\chi_1}{2}\sum_{i=0}^{3}\beta_i\left(\frac{r}{a}\right)^{2i}\right). \tag{43}$$

In the limit when the plate is rigid (i.e. $R \to \infty$), it can be shown that (42) gives

$$w_0 = \frac{P_0(1-\nu_S)}{4G_S a}\left(1 - \frac{P_M}{P_0}\left\{\frac{2}{\pi}\tan^{-1}\left(\frac{a}{c}\right) + \frac{ac}{\pi(1-\nu_S)(a^2+c^2)}\right\}\right), \tag{44}$$

which is in agreement with the exact closed form solution obtained by Selvadurai [12] for the interaction of a rigid punch and a Mindlin force. An important aspect is the development

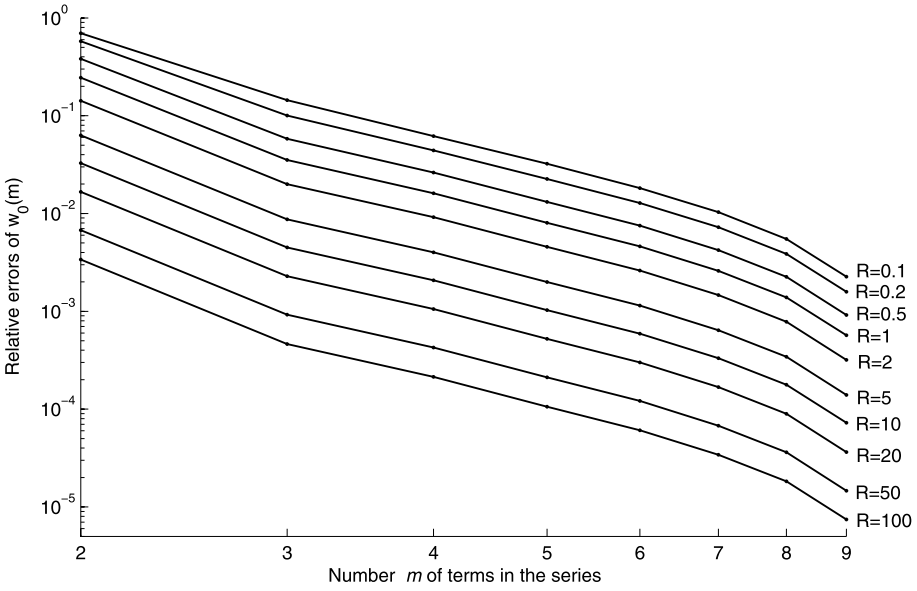

Fig. 3 Relative errors of w_0, for $m = 2, \ldots, 9$ terms in (5), as referred to $m = 10$ terms. The Mindlin force P_M is applied at the depth $c = a$ and the Poisson's ratio is $\nu_S = 0.3$

of an analytical closed form result for a moderately flexible plate, which has practical applications. In order to validate the approximation, either the exact boundary value problem defined by (1) to (4) needs to be solved or the range of applicability of the solution should be assessed by comparison with a computational result [19].

7 Numerical Examples

Adopting consistent units, the plate parameters are $D = 6.0$, $a = 5$, $\nu_P = 0.3$ and the applied loads are $P_0 = P_M = 1$. Ten different values of the geomaterial elastic modulus G_S are selected to correspond to the following values of the relative rigidity:

$$R = \frac{1 - \nu_S}{G_S a^3} D = [0.1, 0.2, 0.5, 1, 2, 5, 10, 20, 50, 100]\,. \tag{45}$$

The following numerical calculations were done with the mathematical software Maple™ with 15 digits accuracy. A convergence study is given in Fig. 3, with log-log representation of relative errors of w_0, given in (16) at $r = 0$ for $m = 2, \ldots, 9$ terms in (5), as referred to the results with $m = 10$ terms, evaluated for 10 different values of the relative rigidity R. The errors decrease almost monotonically with an increase in the number of terms in the series for $w(r)$ and with an increase in the relative rigidity.

For an infinitely rigid plate and $\nu_S = 0.3$, the five-digit numerical values of the normalized displacement $w_0(\times a G_S / P_0)$ are 0.047711 and 0.091515, for P_M applied at $c = a$ and $c = 2a$, respectively. Table 1 shows the corresponding results of w_0 for the rigidity values of (45). Results for $R \geq 50$ are almost indistinguishable from those obtained when $R \to \infty$.

Figure 4 represents the displacement w_0 at $r = 0$ in (5) as functions of the relative rigidity values R of (45) and for different values of the Poisson's ratio: $\nu_S = [0.1,\ 0.2,\ 0.3, 0.4, 0.5]$.

Table 1 Relative results $w_0(R)/w_0(R \to \infty)$ of (16) for $m = 10$ in (5)

	$R = .1$	$R = .2$	$R = .5$	$R = 1$	$R = 2$	$R = 5$	$R = 10$	$R = 20$	$R = 50$	$R = 100$
$c = a$	2.3888	1.8247	1.3744	1.1963	1.1006	1.0409	1.0205	1.0103	1.0041	1.0020
$c = 2a$	3.3123	2.3662	1.6181	1.3237	1.1658	1.0673	1.0338	1.0170	1.0068	1.0034

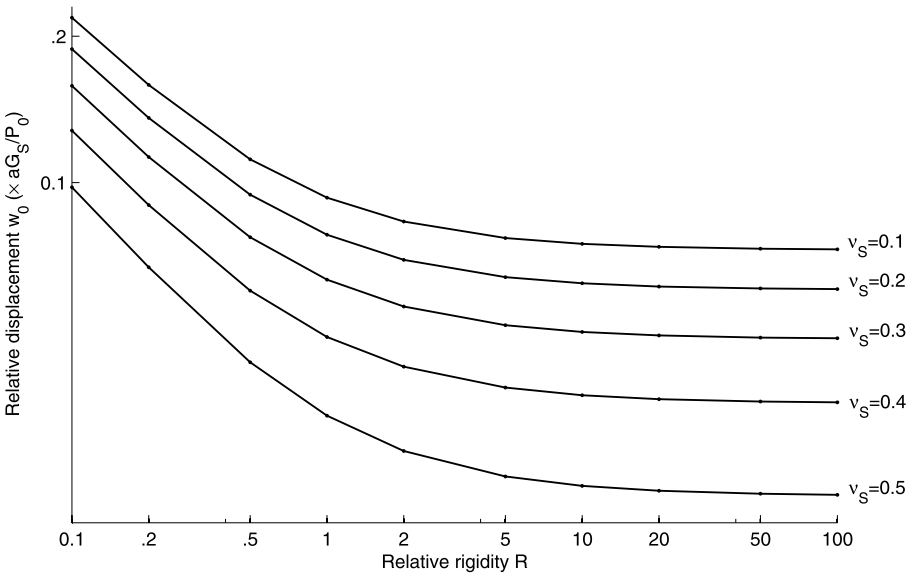

Fig. 4 Displacements w_0 of (16) for P_M applied at $c = a$ and using $m = 10$ terms in (5)

The Mindlin force P_M is applied at the depth $c = a$ and $m = 10$ terms are used in (16). For the same relative rigidity, the displacement w_0 increases significantly as ν_S decreases.

In Fig. 5, displacement values w_0 at $r = 0$ in (16) are shown as functions of the depth c at which P_M is applied and for the different values of the relative rigidity R given in (45). The results are obtained for $\nu_S = 0.3$ and using $m = 10$ terms in (5). An initially significant decrease in w_0 with increasing R is observed.

Figure 6 complements the information of the previous figure, with results shown for three different values of the Poisson's ratio, $\nu_S = [0.1,\ 0.3,\ 0.5]$. Values of w_0 increase as ν_S decreases. Results for $R = 50$ are indistinguishable from those obtained when $R \to \infty$.

Figure 7 illustrates the variation of the displacements $w_r(r)$ of (16) along the radial distance $0 \le r \le a$, as obtained for $m = 10$ terms in (5). All results are normalized by setting $w(0) \equiv w_0 = 1$. The Mindlin force $P_M = P_0$ is applied at the depth $c = a$. Results are given for $R = 0.1$ and for five different values of the Poisson's ratio: $\nu_S = [0.1,\ 0.2,\ 0.3, 0.4, 0.5]$. Similar results are shown in Fig. 8, for a fixed Poisson's ratio $\nu_S = 0.3$ and the different relative rigidity values of (45). As $r \to a$, the relative displacements tend to decrease with decreasing values of R and ν_S. No negative values of $w(r)$, as given in (16), were observed for the parameters selected in the numerical evaluations. Loss of contact between the plate and soil—which is identified as $\sigma_{zz}(r, 0) > 0$ in (11) for $w_r(r)$ given as in (16)—is only observed for very flexible plates and small values of ν_S and c.

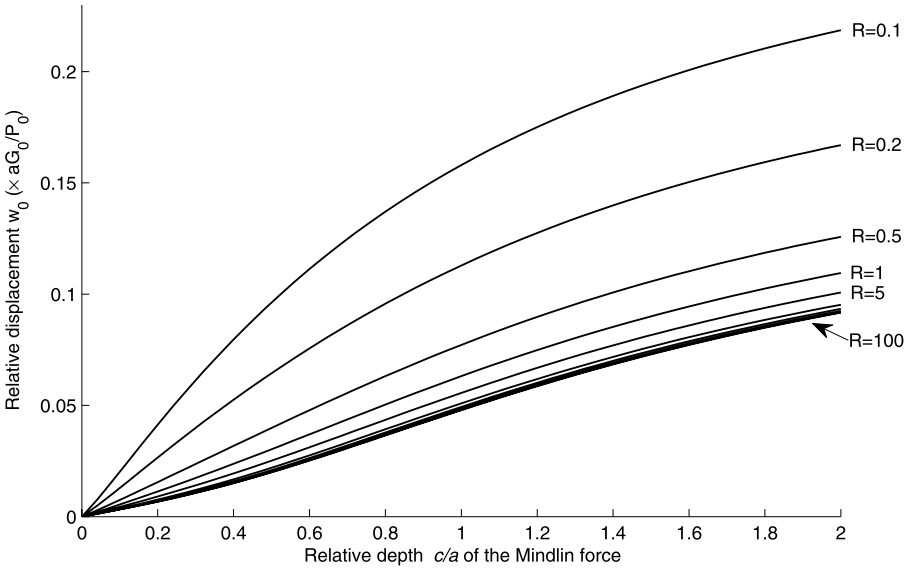

Fig. 5 Displacements w_0 of (16) for $\nu_S = 0.3$ and using $m = 10$ terms in (5)

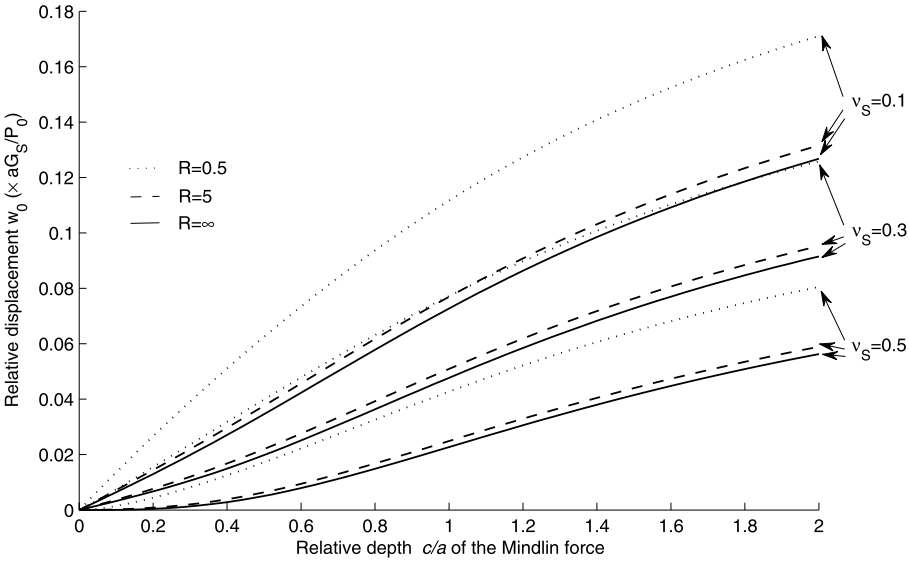

Fig. 6 Displacements w_0 of (16) for $m = 10$ terms in (5) (*dot*, *dash* and *solid line* representations for the relative rigidity values $R = [0.5,\ 5,\ \infty]$)

Concluding Remarks

The paper presents an analytical study of the mechanics of axisymmetric frictionless contact between an isotropic elastic halfspace and a flexible plate, induced by the action of

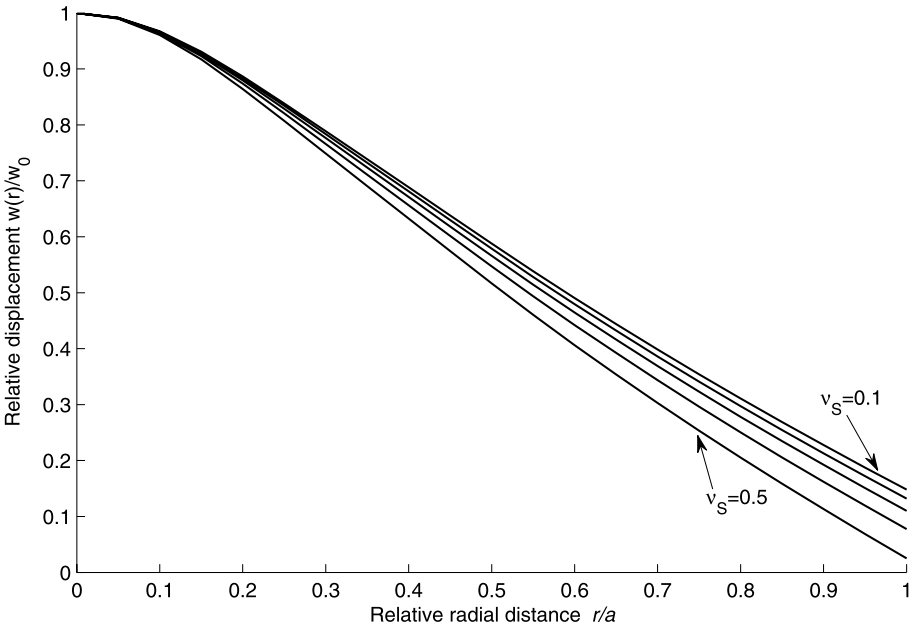

Fig. 7 Relative plate displacements along $0 \leq r \leq a$ for $R = 0.1$ and $P_M = P_0$ applied at $c = a$

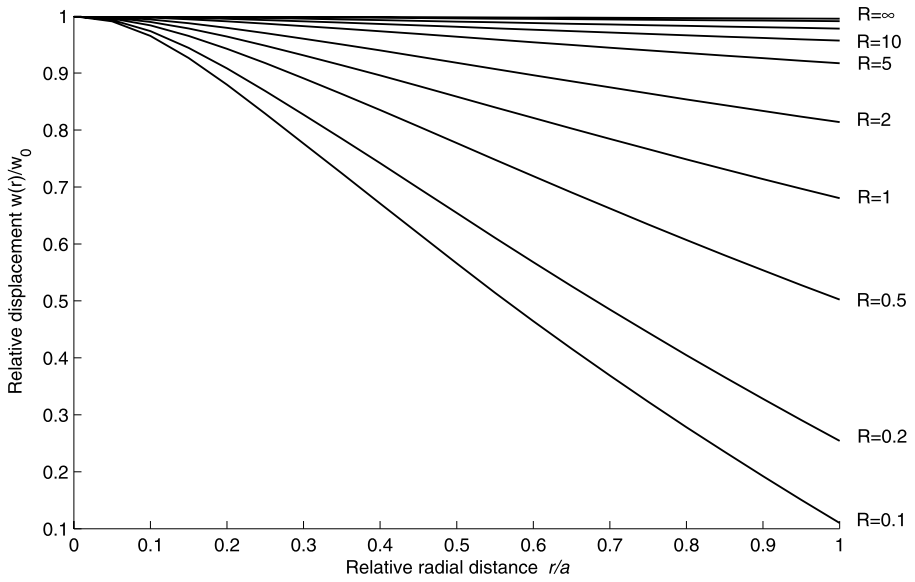

Fig. 8 Relative plate displacements along $0 \leq r \leq a$ for $\nu_S = 0.3$ and $P_M = P_0$ applied at $c = a$

loads applied directly to the plate and a localized Mindlin force applied at the interior of the halfspace region. The analysis uses a variational approach where the deflection of the plate is represented by a power series in the radial coordinate. The solution to the directly loaded

plate serves as the auxiliary solution that can be used in conjunction with the Maxwell-Betti reciprocal theorem to determine the deflection of the plate due to the internally applied Mindlin force. The theoretical developments for the deflection of the flexible plate, which is proposed for estimating the deformability characteristics of a geomaterial region depends, among other parameters, on the relative stiffness between the plate and the geomaterial. The ultimate objective of the plate load test is to determine the bulk properties of the geomaterial. When the plate is rigid, the bulk deformability property (i.e., $G_S/(1-\nu_S)$) can be determined directly using the exact analytical solution for the interaction between the loaded plate and the internal Mindlin force [12]. When the plate is flexible, the estimation of the bulk deformability cannot be made directly since the relative rigidity parameter R influences the measured plate deflection. An approach for parameter extraction is to initially assume the plate to be rigid to obtain a first estimate for the bulk deformability property and to improve the successive estimates for the bulk deformability by accounting for the relative rigidity parameter R.

Acknowledgements The authors would like to thank the reviewer for comments that lead to the improvement of the presentation. The work described in this paper was supported by a NSERC Discovery grant awarded to the first author, who also would like to thank the hospitality of PUC-Rio during the research collaborations. The second author acknowledges the support of the Brazilian agencies CNPq and FAPERJ.

Appendix

In the implementation proposed in Sect. 5, the coefficients of the matrix $\mathbf{M}$ in (18) that corresponds to the cross-sectional forces of (2) may be generated as

$$M_{ij} = \begin{bmatrix} M_{rr_j} \\ Q_{rr_j} \end{bmatrix} = D \begin{bmatrix} -(2j-2)(2j-3+\nu_P)\,\xi^{2j-4}/a \\ -8(j-1)^2(j-2)\,\xi^{2j-3}/a^2 \end{bmatrix}. \tag{A.1}$$

The coefficients of the plate stiffness matrix $\mathbf{K}_P$ defined in (22) are expressed as

$$K_{P_{ij}} = \begin{cases} = 0, & \text{if } i=1 \text{ or } j=1, \\ = 8\pi D(i-1)(j-1)\left(\frac{2(i-1)(j-1)}{i+j-3} - 1 + \nu_P\right). \end{cases} \tag{A.2}$$

For $m=7$ in (5), the halfspace stiffness matrix $\mathbf{K}_{HS}$, as symbolically generated using the mathematical software Maple™, is

$$\mathbf{K}_{HS} = \frac{4G_S a^3}{1-\nu_S} \begin{bmatrix} 1 & \frac{2}{3} & \frac{8}{15} & \frac{16}{35} & \frac{128}{315} & \frac{256}{693} & \frac{1024}{3003} & \frac{2048}{6435} \\ \frac{2}{3} & \frac{4}{5} & \frac{16}{21} & \frac{32}{45} & \frac{256}{385} & \frac{512}{819} & \frac{2048}{3465} & \frac{4096}{7293} \\ \frac{8}{15} & \frac{16}{21} & \frac{64}{81} & \frac{128}{165} & \frac{1024}{1365} & \frac{2048}{2835} & \frac{8192}{11781} & \frac{16384}{24453} \\ \frac{16}{35} & \frac{32}{45} & \frac{128}{165} & \frac{256}{325} & \frac{2048}{2625} & \frac{4096}{5355} & \frac{16384}{21945} & \frac{32768}{45045} \\ \frac{128}{315} & \frac{256}{385} & \frac{1024}{1365} & \frac{2048}{2625} & \frac{16384}{20825} & \frac{32768}{41895} & \frac{131072}{169785} & \frac{262144}{345345} \\ \frac{256}{693} & \frac{512}{819} & \frac{2048}{2835} & \frac{4096}{5355} & \frac{32768}{41895} & \frac{65536}{83349} & \frac{262144}{334719} & \frac{524288}{675675} \\ \frac{1024}{3003} & \frac{2048}{3465} & \frac{8192}{11781} & \frac{16384}{21945} & \frac{131072}{169785} & \frac{262144}{334719} & \frac{1048576}{1334025} & \frac{2097152}{2675673} \\ \frac{2048}{6435} & \frac{4096}{7293} & \frac{16384}{24453} & \frac{32768}{45045} & \frac{262144}{345345} & \frac{524288}{675675} & \frac{2097152}{2675673} & \frac{4194304}{5337189} \end{bmatrix}. \tag{A.3}$$

Moreover, the row vector $\mathbf{s}$ that enters in the matrix definition of the surface stress $\sigma_{zz}(r,0)$ in (27) is

$$\mathbf{s} = \Bigg[1 \; 4\xi^2 - 2 \; \frac{8\xi^4 - 4\xi^2 - 1}{9/8} \; \frac{16\xi^6 - 8\xi^4 - 2\xi^2 - 1}{25/16} \; \frac{128\xi^8 - 64\xi^6 - 16\xi^4 - 8\xi^2 - 5}{1225/128} \; \frac{256\xi^{10} - 128\xi^8 - 32\xi^6 - 16\xi^4 - 10\xi^2 - 7}{3969/256} \; \frac{1024\xi^{12} - 512\xi^{10} - 128\xi^8 - 64\xi^6 - 40\xi^4 - 28\xi^2 - 21}{53361/1024} \; \frac{2048\xi^{14} - 1024\xi^{12} - 256\xi^{10} - 128\xi^8 - 80\xi^6 - 56\xi^4 - 42\xi^2 - 33}{184041/2048}\Bigg], \tag{A.4}$$

where $\xi = r/a$. In this case, the vectors $\mathbf{u}_1$ and $\mathbf{u}_2$ of the matrix expression of the displacement in (28) can be evaluated as

$$\mathbf{u}_1 = \Bigg[\frac{\alpha}{4\epsilon} \; \frac{\epsilon\alpha - 4}{-2} \; \frac{3\epsilon^3\alpha - 12\epsilon^2 + 4}{9/2} \; \frac{15\epsilon^5\alpha + 20\epsilon^2 - 60\epsilon^4 - 12}{-75/4} \; \frac{105\epsilon^7\alpha - 420\epsilon^6 + 60 - 84\epsilon^2 + 140\epsilon^4}{3675/32} \; \frac{315\epsilon^9\alpha + 420\epsilon^6 - 252\epsilon^4 - 140 + 180\epsilon^2 - 1260\epsilon^8}{-19845/64} \; \frac{3465\epsilon^{11}\alpha - 13860\epsilon^{10} - 1540\epsilon^2 + 4620\epsilon^8 + 1260 - 2772\epsilon^6 + 1980\epsilon^4}{800415/256} \; \frac{45045\epsilon^{13}\alpha + 16380\epsilon^2 - 20020\epsilon^4 - 36036\epsilon^8 + 60060\epsilon^{10} - 180180\epsilon^{12} - 13860 + 25740\epsilon^6}{-19324305/512}\Bigg], \tag{A.5}$$

$$\mathbf{u}_2 = \frac{1}{1+\epsilon^2}\Bigg[1 \; \epsilon(\epsilon^2+1)\alpha - 4\epsilon^2 - 2 \; \frac{3\epsilon^3(\epsilon^2+1)\alpha + 1 - 8\epsilon^2 - 12\epsilon^4}{-9/8} \; \frac{15\epsilon^5(\epsilon^2+1)\alpha + 8\epsilon^2 - 40\epsilon^4 - 60\epsilon^6 - 2}{25/8} \; \frac{210\epsilon^7(\epsilon^2+1)\alpha - 48\epsilon^2 - 560\epsilon^6 + 112\epsilon^4 - 840\epsilon^8 + 15}{-3675/128} \; \frac{315\epsilon^9(\epsilon^2+1)\alpha - 840\epsilon^8 - 1260\epsilon^{10} + 40\epsilon^2 - 14 - 72\epsilon^4 + 168\epsilon^6}{3969/128} \; \frac{3465\epsilon^{11}(\epsilon^2+1)\alpha + 105 - 13860\epsilon^{12} - 9240\epsilon^{10} - 280\epsilon^2 + 1848\epsilon^8 - 792\epsilon^6 + 440\epsilon^4}{-266805/1024} \; \Bigg(\frac{45045\epsilon^{13}(\epsilon^2+1)\alpha + 24024\epsilon^{10} + 2520\epsilon^2 - 120120\epsilon^{12} - 10296\epsilon^8}{2760615/1024} + \frac{5720\epsilon^6 - 180180\epsilon^{14} - 3640\epsilon^4 - 990}{2760615/1024}\Bigg)\Bigg], \tag{A.6}$$

where $\epsilon = z/a$ and $\alpha = \pi - 2\arctan(\frac{\epsilon^2-1}{2\epsilon})$.

References

1. Barber, J.R.: Elasticity. Kluwer Academic, Dordrecht (2004)
2. Boussinesq, J.: Applications des Potentiels. Gauthier-Villars, Paris (1885)
3. Carlson, D.E.: Linear thermoelasticity. In: Truesdell, C. (ed.) Handbuch der Physik, vol. VIa/2, pp. 297–345. Springer, Berlin (1972)
4. Coulson, C.A.: Suggested methods for determining in situ deformability of rock. Int. J. Rock Mech. Min. Sci. **16**, 195–214 (1979)
5. Davis, R.O., Selvadurai, A.P.S.: Elasticity and Geomechanics. Cambridge University Press, Cambridge (1996)
6. Galin, L.A.: Contact Problems in the Theory of Elasticity. North Carolina State College, Raleigh (1961). Translated from Russian by H. Moss, edited by I.N. Sneddon
7. Gladwell, G.M.L.: Contact Problems in the Classical Theory of Elasticity. Sijthoff and Noordhoff, Alphen aan den Rijn, The Netherlands (1980)
8. Green, A.E.: On Boussinesq's problem and penny-shaped cracks. Proc. Camb. Philos. Soc. **45**, 251–257 (1949)
9. Harding, J.W., Sneddon, I.N.: The elastic stresses produced by the indentation of the plane surface of a semi-infinite elastic solid by a rigid punch. Proc. Camb. Philos. Soc. **41**, 16–26 (1945)
10. Jaeger, C.: Rock Mechanics and Engineering. Cambridge University Press, Cambridge (1972)
11. Mindlin, R.D.: Force at a point in the interior of a semi-infinite solid. Physics **7**, 195–202 (1936)
12. Selvadurai, A.P.S.: The interaction between a rigid circular punch on an elastic halfspace and a Mindlin force. Mech. Res. Commun. **5**, 57–64 (1978)
13. Selvadurai, A.P.S.: The displacement of a rigid circular foundation anchored to an isotropic elastic halfspace. Geotechnique **29**, 195–202 (1979)
14. Selvadurai, A.P.S.: Elastic Analysis of Soil-Foundation Interaction. Developments in Geotechnical Engineering, vol. 17. Elsevier, Amsterdam (1979)
15. Selvadurai, A.P.S.: The interaction between a uniformly loaded circular plate and an isotropic elastic halfspace: a variational approach. J. Struct. Mech. **7**, 231–246 (1979)
16. Selvadurai, A.P.S.: Elastic contact between a flexible circular plate and a transversely isotropic elastic halfspace. Int. J. Solids Struct. **16**, 167–176 (1980)
17. Selvadurai, A.P.S.: The Biharmonic Equation, Poisson's Equation. Partial Differential Equations in Mechanics, vol. 2. Springer, Berlin (2000)
18. Selvadurai, A.P.S.: The analytical method in geomechanics. Appl. Mech. Rev. **60**, 87–106 (2007)
19. Selvadurai, A.P.S., Dumont, N.A., Oliveira, M.F.F.: Mindlin's problem for a halfspace with a surface constraint. In: Proceedings of PACAM XI—11th Pan-American Congress of Applied Mechanics (2010). (6 pp. on CD)
20. Sneddon, I.N.: The relation between load and penetration in the axisymmetric Boussinesq problem for a punch of arbitrary profile. Int. J. Eng. Sci. **3**, 47–57 (1965)
21. Uflyand, Y.S.: Survey of Articles on the Application of Integral Transforms in the Theory of Elasticity. North Carolina State College, Raleigh (1965). Translated from Russian by W.J.A. Whyte, edited by I.N. Sneddon
22. Zienkiewicz, O.C., Stagg, K.G.: Cable method of in-situ rock testing. Int. J. Rock Mech. Min. Sci. **4**, 273–300 (1967)